ARTIFICIAL SATELLITES, Vol. 48, No. 3 – 2013
DOI: 10.2478/arsa-2013-0010

ANALYSIS OF CURRENT POSITION DETERMINATION ACCURACY IN NATURAL RESOURCES CANADA PRECISE POINT POSITIONING SERVICE

Grzegorz Krzan, Karol Dawidowicz, Krzysztof Świątek
University of Warmia and Mazury in Olsztyn, Faculty of Geodesy and Land Management, Institute of Geodesy, 10-719 Olsztyn, ul. Oczapowskiego 1
g.krzan@gmail.com, karol.dawidowicz@uwm.edu.pl, krzysztof.swiatek@uwm.edu.pl

ABSTRACT. Precise Point Positioning (*PPP*) is a technique used to determine high-precision position with a single *GNSS* receiver. Unlike *DGPS* or *RTK*, satellite observations conducted by the *PPP* technique are not differentiated, therefore they require that parameter models should be used in data processing, such as satellite clock and orbit corrections. Apart from explaining the theory of the *PPP* technique, this paper describes the available web-based online services used in the post-processing of observation results. The results obtained in the post-processing of satellite observations at three points, with different characteristics of environment conditions, using the *CSRS-PPP* service, will be presented as the results of the experiment. This study examines the effect of the duration of the measurement session on the results and compares the results obtained by working out observations made by the *GPS* system and the combined observations from *GPS* and *GLONASS*. It also presents the analysis of the position determination accuracy using one and two measurement frequencies.

Key words: Satellite geodesy, *PPP, CSRS, GPS, GLONASS*

1. INTRODUCTION

Currently, differential techniques are the most commonly-used method in geodesic measurements in countries with well-developed reference station infrastructure. Their high precision is ensured by corrections calculated with the use of *GNSS* receivers at reference stations which are broadcast in real time to the user's receiver, or taken into account at the post-processing stage. Due to the high costs of establishing and maintaining a network of permanent stations, as well as the fact that highly precise satellite orbits, clock corrections and atmospheric products are made available by such centres as the *International GNSS Service* (*IGS*), the *Center for Orbit Determination for Europe* (*CODE*) and the *Jet Propulsion Laboratory* (*JPL*), many research programmes studying the *PPP* (*Precise Point Positioning*) technique have been undertaken in recent years (Alcay et al., 2012).

The *PPP* technique uses observations from a single *GNSS* receiver, which can achieve a precision in the order of several centimetres (Mireault et al., 2012; Bisnath et al., 2003). However, observations from a base station are not used, which prevents the distance from the station from restricting the range of measurements made by the user (Huber et al., 2010; Rizos

2010). On the other hand, an absence of differentiation of observations necessitates using precise satellite orbits and clock corrections in the post-processing of results as well as modelling iono- and tropospheric refractions, solid earth and ocean tides, antenna phase-center offsets and variations, carrier-phase wind-up, relativistic effects, etc. (Mireault et al., 2012). The impact of these factors is determined from continuous satellite observations by those services (e.g. solid earth and ocean tides) or by laboratory tests (antenna phase-center offsets and variations, carrier-phase wind-up). The ambiguity of phase measurements is also a certain barrier. As a standard, the *PPP* technique employs a *float*-type solution, which requires long observations (over 20 minutes) to achieve a precision of several centimetres. It is expected that the time will be reduced significantly when signals from the *Galileo* and *Beidou* systems are used in satellite measurements (Rizos et al., 2012). This should happen owing to the possibility of creating additional linear combinations of code and phase observations, based on 3-5 different frequencies. Linear combinations of phase and code measurements, created now with the use of two frequencies, allow for elimination from a measurement of the ionospheric refraction effect and the real-valued carrier phase ambiguity terms estimated from the measurement model (Bisnath et al., 2008).

The theoretical foundations of the *PPP* method were formulated by Zumberge et al. (1997). The observational equations for code and phase measurements, made at two frequencies, have the following form (Hofmann-Wellenhof et al., 2008):

$$P = \rho + cdt_r + cdt_b + \Delta_{trp} + \Delta_{ion} + \varepsilon \tag{1}$$

$$\phi = \rho + cdt_r + cdt_b + \lambda N + \Delta_{trp} - \Delta_{ion} + \varepsilon \tag{2}$$

where:
P – pseudo-range between satellite and receiver;
Φ – difference between the phases of signals in the moment t;
ρ – geometric distance between satellite and receiver;
c – speed of light;
dt_r – difference between time of signal transmission and signal reception;
dt_b – difference between satellite and receiver clock biases;
Δ_{trp} – tropospheric delay;
Δ_{ion} – ionospheric delay;
λ – wavelength;
N – phase ambiguity;
ε – other errors.

The process of determination of coordinates of a receiver in the *PPP* method employs ephemeris corrections determined with a high precision and satellite clock corrections to reduce their effect on the post-processing results. Subsequently, if a measurement is made with a two-frequency receiver, an *ionosphere-free* linear combination is used (Cai et al., 2007; Kouba et al., 2001):

- for code measurements:

$$P_{IF} = \frac{P_1 f_1^2 - P_2 f_2^2}{f_1^2 - f_2^2} = \rho + cdt_r + \Delta_{trp} \tag{3}$$

- for phase measurements:

$$\phi_{IF} = \frac{\lambda_1 \phi_1 f_1^2 - \lambda_2 \phi_2 f_2^2}{f_1^2 - f_2^2} = \rho + cdt_r + \Delta_{trp} + \frac{\lambda_1 N_1 f_1^2 - \lambda_2 N_2 f_2^2}{f_1^2 - f_2^2} \tag{4}$$

The *ionosphere-free* linear combination makes it possible to completely eliminate the first order ionosphere delay. Therefore, unknown parameters to be determined in the equations include: the position of a receiver contained in ρ, receiver clock offset, tropospheric refraction delay Δ_{trp} and the value of the ambiguity of phase measurements N. However, the combination is considerably noised due to an increase in the effect of the multi-path nature and the receiver errors on the measurement results (Van Der Marel et al., 2012).

If a measurement is performed at one frequency, it is impossible to create an *ionosphere-free* linear combination. The effect of the ionosphere in such cases is reduced by one of two methods:

- with a linear combination of frequency *L1* for code and phase measurements:

$$\phi_{IF} = 0.5 \cdot P_1 + 0.5 \cdot \phi_1 = \rho + cdt_r + \Delta_{trp} + \frac{1}{2}\lambda_1 N_1 + \varepsilon \quad (5)$$

which eliminates the tropospheric delay and reduces the noises of code observations by half;

- with the ionospheric delays determined from ionospheric maps, e.g. *GIM* (*Global Ionosphere Maps*) developed by *IGS*.

Slant tropospheric delay is expressed as a function of the *Zenith Tropospheric Delay (ZTD)* (which is an estimated parameter in the *PPP* method) with the use of the mapping function (Stępniak et al., 2012).

2. ONLINE *PPP* SERVICES

Web-based *PPP* services provide a quick, practical alternative for software used for the post-processing of satellite observations by a user. Post-processing of measurements in online services is done automatically and a user only needs to set the basic post-processing parameters and upload a file in the *RINEX* format. Individual services differ mainly in processing algorithms, the origin of the error models used in post-processing as well as the form of making the processing results available. The most popular *PPP* services are:

- *APPS* provided by *JPL California Institute of Technology* (https://apps.gdgps.net/), which uses models of orbits and clock corrections from its own system *JPL's GDGPS*; *RINEX* files can be uploaded to the service from the Internet site or uploaded to the FTP server; after the results have been processed, the coordinates are provided in the *ITRF2008* system; the service allows users to perform the post-processing of static and kinematic observations at two frequencies; observations from the *GLONASS* system are not used in post-processing;

- *CSRS-PPP* provided by *Natural Resources Canada* (http://www.geod.nrcan.gc.ca/), which uses models of orbits and clock corrections developed by the *IGS* services; *RINEX* or *CompactRINEX* files can be uploaded from the website or through the *PPP Direct* software, made available by the service; after post-processing, the user receives not only the coordinates and their sigmas in the *ITRF2008* or *NAD83* system, but also diagrams of the visibility of satellites, the temporal convergence of coordinates, estimated tropospheric delay and clock offset as well as detailed observational data from each measurement epoch, etc. *CSRS-PPP* allows for post-processing static and kinematic observations, as well as using observations from the *GLONASS* system;

- other services, such as: *GAPS v5.0* (http://gaps.gge.unb.ca/indexv2.php), *AUSPOS- Online GPS Processing Service* (http://ga.gov.au/bin/gps.pl), *Trimble CenterPoint RTX* (http://trimblertx.com/).

3. METHODOLOGY

The post-processing of observations for this paper was performed with the use of the *CSRS-PPP* (V 1.05 03812) service, which enables a quick, practical method of uploading *RINEX* files by means of the *PPP Direct* program. The service was chosen because of the form of results provided, which allows for detailed analysis of the course of post-processing and for including measurements from the *GLONASS* system in post-processing. The post-processing covered round-the-clock observations made over three consecutive days at 3 points with different characteristics of horizon visibility. Observations made at the *KROL* reference station of the *ASG-EUPOS* system in Olsztyn (Poland) were taken as measurements at point A, assuming that this is the point with the optimum conditions for observations, which is a consequence of a totally unobscured horizon. Points B and C were marked near typical rural built-up areas, single trees and other objects which reduce the number of visible satellites and favour the multi-path effect (Fig. 1 and 2).

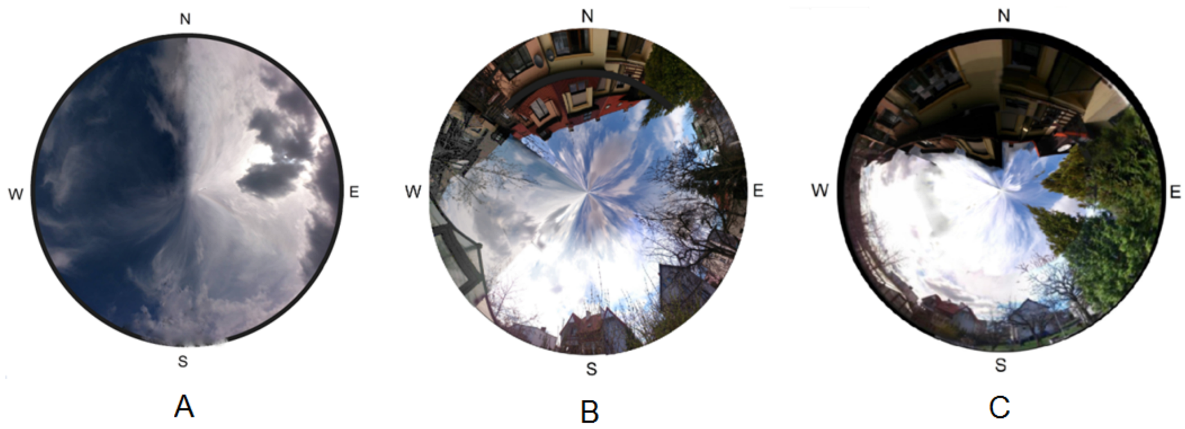

Fig. 1. Horizon visibility from points A, B, C

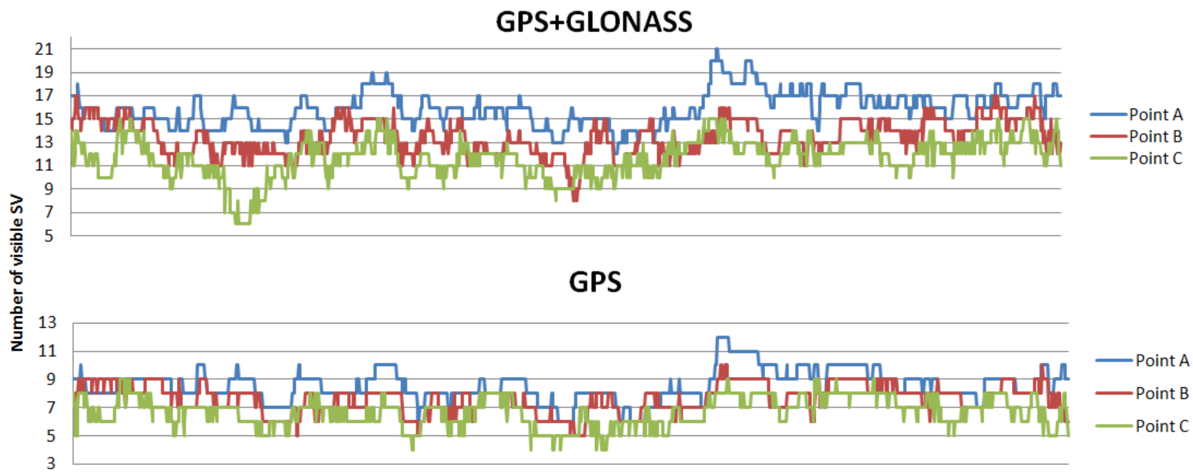

Fig. 2. Daily changes of satellite visibility at points A, B, C during the observations

The effect of terrain obstacles on the visibility of satellites can be seen in this diagram. In extreme cases, the number of the satellites observed at point A is up to three times larger than at point C during the same measurement epoch. The average number of satellites observed at points A, B and C was 15, 13, 11 for variant *GPS+GLONASS* and 8, 7, 6 for variant *GPS,* respectively.

Measurements at the *KROL* station were performed with a *Javad TRE_G3TH Sigma* receiver with *JAV_GRANT-G3T JAVC* antenna (*www.asgeupos.pl*), while at points B and C – with a *Topcon HiperPRO* receiver with *TPSHIPER_PLUS antenna*.

72 hours of observations performed with a 1-second interval were divided into 4 time variants (0.5h, 1h, 2h, 4h) and into 4 variants depending on the observed signals (observations

at frequencies *L1* and *L1+L2* and using signals from the *GPS* and *GPS+GLONASS* systems), with the use of the *TEQC* software and the author's own scripts, written in the C# language. This produced: 144 half-hour sessions, 72 hour-long sessions, 36 two-hour sessions and 18 four-hour sessions. Post-processing was performed with the use of the most precise "final" *IGS* products; results were obtained in the *ITRF2008* frame and in *UTM* geographic coordinate system. Table 1 contains the most important *NRCan PPP* software processing options and parameters.

Tab. 1. *NRCan PPP* software processing options and parameters
(source: *http://www.geod.nrcan.gc.ca/*)

Option	L1	L1&L2
User Selected		
User dynamics	Static or Kinematic	Static or Kinematic
Reference frame	*ITRF* or *NAD83*(*CSRS*)	*ITRF* or *NAD83*(*CSRS*)
From RINEX Header		
Frequency observed	as defined by the RINEX RECORD '# / TYPES OF OBSERV'	
Marker to ARP distance	as defined by the RINEX RECORD 'ANTENNA: DELTA H/E/N'	
Type of Antenna	as defined by the RINEX RECORD 'ANT # / TYPE'	
Preset by application		
Observation processed	Code	Code and Phase
Satellite orbits	Precise	Precise
Satellite clocks	5-minute(*)	5-minute(*)
Ionospheric model	IONEX	L1 and L2
Marker coordinates	Estimated	Estimated
Tropospheric delay	Modeled	Estimated
Clock interpolation	Yes	Yes
Parameter smoothing	No	Yes if kinematic
Coordinate system	Ellipsoidal	Ellipsoidal
Pseudorange A-PRIORI sigma	2.000 m	2.000 m
Carrier phase A-PRIORI sigma	0.100 m	0.010 m
Cutoff elevation	10.000 deg	10.000 deg

An analysis of the results presented in this paper shows differences of coordinates (*northing, easting, elevation*) for different variants of post-processing. The aim of the work was to attempt to determine the usability of the *PPP* method in geodesic measurements.

4. THE RESULTS OF THE EXPERIMENT

The following Tables and diagrams show the results of post-processing for different variants of elaborations. The horizontal coordinates of points are presented in the Universal Transverse Mercator (*UTM)* system of zone 34U (scale factor: 0.99961396) (Fig. 3, 5, 7, 9, 11, 13). Table 2 presents observational statistic (number of processed observations and observations rejected) for each variants. Because of the very large number of sessions in individual variants Table 2 contains only the mean values. The large number of rejected observations on point A is probably due to the fact that for ASG-EUPOS stations the 0˚ degrees elevation cutoff angle is adopted. Points B and C were measured with 10˚ degrees cutoff angle - the same as in CSRS service is adopted. There is also visible that generally there are not differences in the number of observations processed or rejected when L1+L2 and L1 variants are compared. It is probably due to the fact that when L1+L2 observations are used the so called L3 observations are created (and these are counted in the statistics).

Tables 3 and 4 present standard deviations and the maximum deviations of coordinates from their real values, which are adopted as average coordinates from three 24-hour solutions obtained from the most precise variant (*GPS+GLONASS; L1+L2*).

Tab. 2. Observational statistic for all processing variants.

Processing variant	***GNSS* system**	**Point A**		**Point B**		**Point C**	
		Processed obs.	***Rejected obs.***	***Processed obs.***	***Rejected obs.***	***Processed obs.***	***Rejected obs.***
		0.5 h sessions					
GPS+GLONASS L1+L2	***GPS***	15215	5228	13418	782	11791	904
	GLONASS	13336	2896	10637	415	8932	328
GPS+GLONASS L1	***GPS***	15215	5228	13895	298	12399	296
	GLONASS	13338	2894	10963	84	9251	9
GPS L1+L2	***GPS***	15214	5228	13416	782	11794	904
GPS L1	***GPS***	15215	5228	13899	298	12402	296
		1.0 h sessions					
GPS+GLONASS L1+L2	***GPS***	30413	10461	26833	1567	23565	1806
	GLONASS	26675	5770	21279	818	17859	662
GPS+GLONASS L1	***GPS***	30413	10461	27787	601	24775	597
	GLONASS	26678	5767	21383	175	17872	17
GPS L1+L2	***GPS***	30413	10461	26829	1571	23569	1808
GPS L1	***GPS***	30413	10461	27795	601	24779	597
		2.0 h sessions					
GPS+GLONASS L1+L2	***GPS***	60788	20967	53654	3132	47112	3612
	GLONASS	53330	11635	42456	1660	35659	1288
GPS+GLONASS L1	***GPS***	60788	20967	55560	1201	49518	1194
	GLONASS	53335	11630	43756	339	36900	35
GPS L1+L2	***GPS***	60788	20967	53647	3138	47106	3617
GPS L1	***GPS***	60788	20967	55575	1201	49527	1194
		4.0 h sessions					
GPS+GLONASS L1+L2	***GPS***	121544	41886	107284	6382	94335	7194
	GLONASS	106621	23322	84819	3253	71259	2593
GPS+GLONASS L1	***GPS***	121544	41885	111243	2372	99148	2357
	GLONASS	106631	23311	87363	664	73750	79
GPS L1+L2	***GPS***	121543	41886	107263	6393	94331	7198
GPS L1	***GPS***	121544	41885	111279	2372	99167	2357

The standard deviation at point A for half-hour measurement sessions was equal to approx. 0.03 m for the northing coordinate, approx. 0.06 m for the easting coordinate and approx. 0.06 m for elevation. The values for points with limited horizon visibility (B, C) are accordingly higher and they range from approx. 0.05 m (northing, point B) to as much as 0.22 m (elevation, point C). The maximum deviations of coordinates from the “real” value for half-hour sessions range from 0.118 to 0.233 m (point A), up to almost 1.4 m (point C). The values decrease approximately in proportion to the duration of the measurement session. Doubling the duration of a session resulted in reducing the standard deviation and the maximum deviations of coordinates from the “real” values by half. Adding observations from the *GLONASS* system to the post-processing decreased the standard deviation values for sessions lasting up to 2 hours, especially at point C, but in many cases maximum deviations has increased. Extending the session duration to 4 hours in this variant did not result in any considerable improvement and in most cases even slightly worsened results. Maybe this is due to a lower accuracy of *GLONASS* corrections that have to be applied in post-processing. For example *GLONASS* precise orbits are at 10-15 cm and clock data at the 1.5 ns level of accuracy. For *GPS* these values are respectively: less than 5 cm for precise orbits and 0.1 ns for clock data. The problem is undoubtedly very interesting and is worthy of further study.

Tab. 3. Standard deviations and maximum deviations for post-processing of *L1+L2*

L1+L2			0.5 h		1 h		2 h		4 h	
			σ	max dev.	σ	max dev.	σ	max dev.	σ	max dev.
Point A	North	*GPS+GLONASS*	0.028	0.129	0.013	0.046	0.007	0.017	0.006	0.017
		GPS	0.032	0.118	0.018	0.046	0.009	0.024	0.006	0.012
	East	*GPS+GLONASS*	0.051	0.233	0.039	0.087	0.021	0.082	0.016	0.058
		GPS	0.068	0.207	0.036	0.100	0.017	0.045	0.010	0.022
	Height	*GPS+GLONASS*	0.053	0.195	0.031	0.112	0.023	0.106	0.020	0.074
		GPS	0.062	0.208	0.034	0.087	0.019	0.048	0.007	0.013
Point B	North	*GPS+GLONASS*	0.047	0.226	0.027	0.134	0.010	0.027	0.006	0.018
		GPS	0.047	0.143	0.023	0.074	0.012	0.028	0.007	0.015
	East	*GPS+GLONASS*	0.095	0.469	0.054	0.257	0.027	0.104	0.016	0.046
		GPS	0.137	0.540	0.067	0.163	0.030	0.096	0.011	0.022
	Height	*GPS+GLONASS*	0.101	0.499	0.050	0.127	0.028	0.058	0.021	0.046
		GPS	0.126	0.405	0.052	0.161	0.032	0.118	0.015	0.029
Point C	North	*GPS+GLONASS*	0.089	0.432	0.048	0.152	0.033	0.097	0.013	0.035
		GPS	0.157	1.253	0.077	0.207	0.039	0.126	0.010	0.017
	East	*GPS+GLONASS*	0.130	0.413	0.073	0.261	0.041	0.097	0.026	0.059
		GPS	0.204	1.211	0.136	0.485	0.047	0.122	0.019	0.039
	Height	*GPS+GLONASS*	0.152	0.603	0.068	0.180	0.048	0.166	0.025	0.050
		GPS	0.225	1.391	0.103	0.357	0.058	0.146	0.031	0.056

An analysis of the diagrams (Fig. 3, 4, 5, 6, 7, 8) has confirmed the results of post-processing shown in Table 3. The diagrams of 2-dimentional coordinates (Fig. 3, 5, 7) are stretched in the east-west direction, which means greater coordinates determination deviations in this plane.

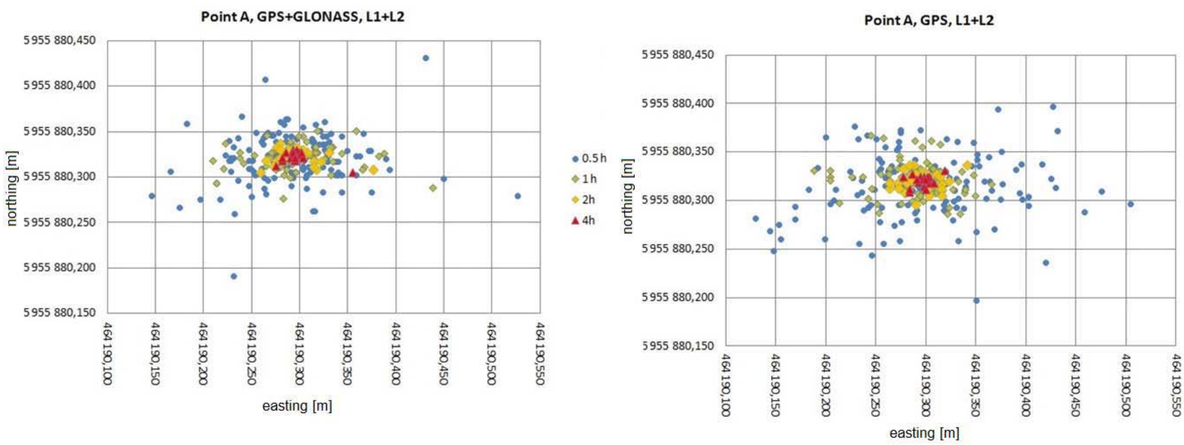

Fig. 3. *UTM* coordinates of point A obtained in the post-processing of observations at two frequencies

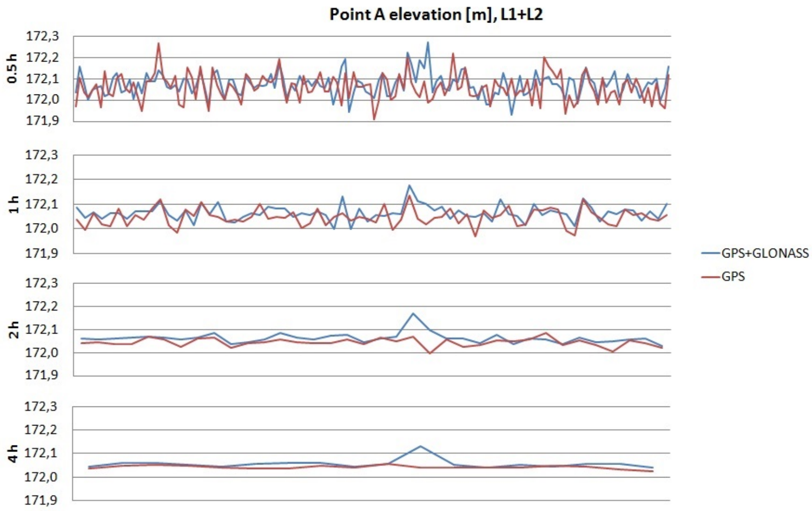

Fig. 4. Elevation of point A obtained in the post-processing of observations at two frequencies

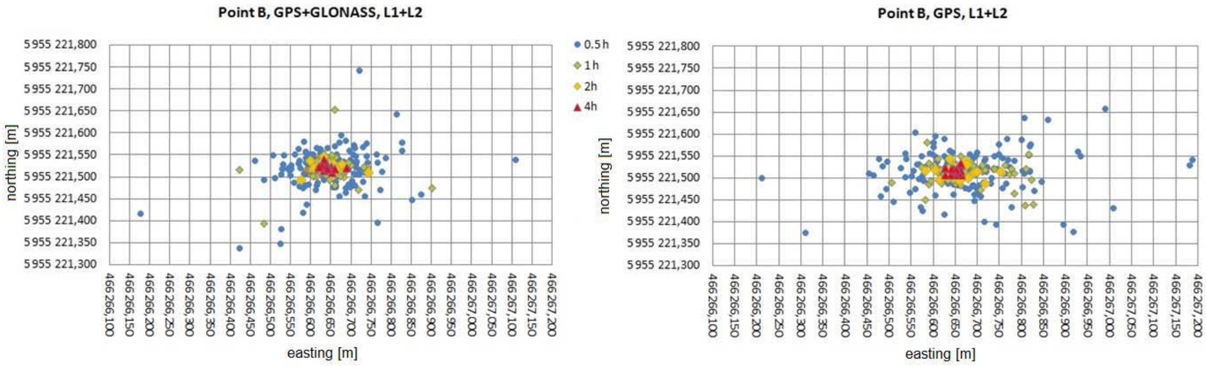

Fig. 5. *UTM* coordinates of point B from the post-processing of observations *L1* and *L2*

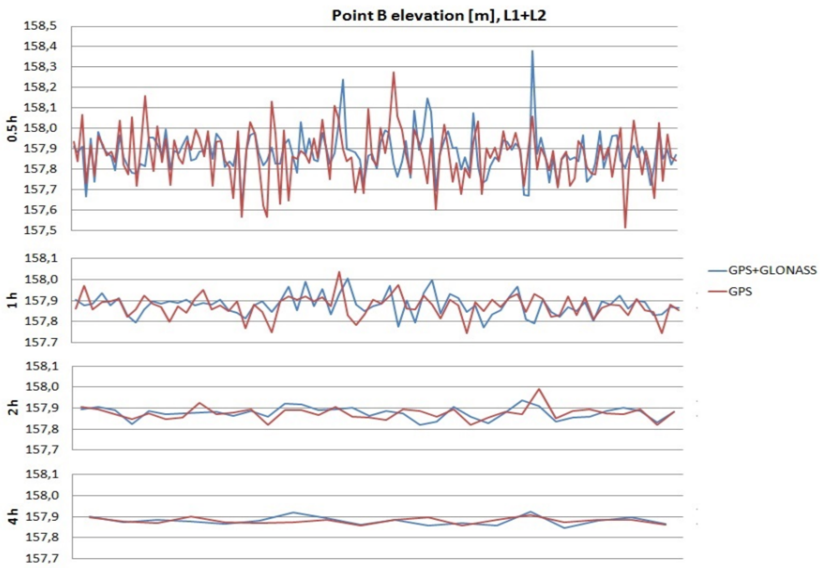

Fig. 6. Elevation of point B obtained in the post-processing of observations at two frequencies

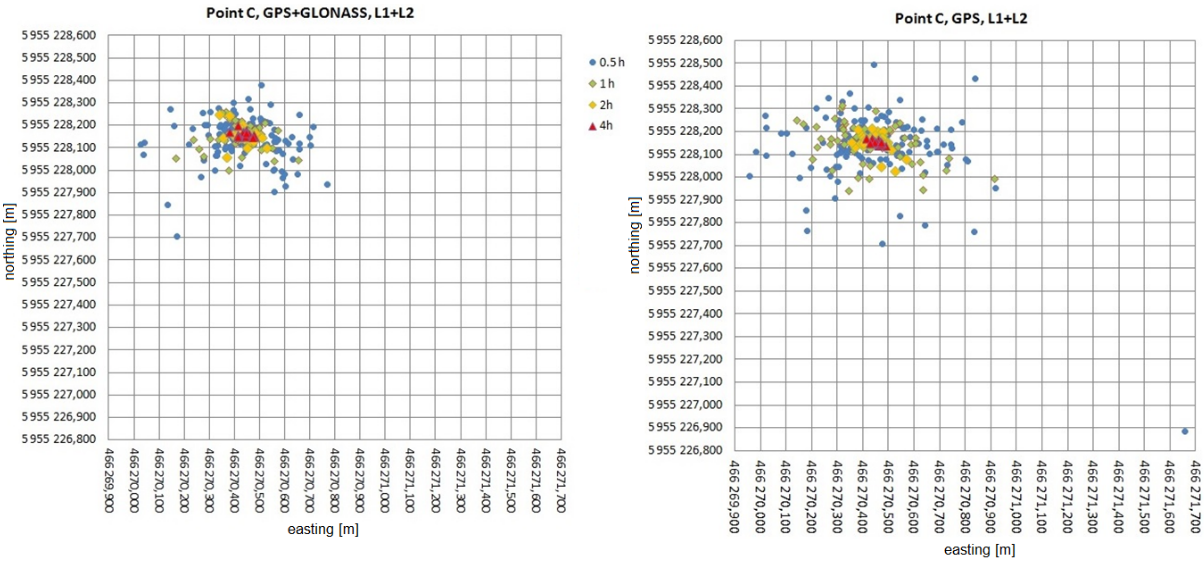

Fig. 7. *UTM* coordinates of point C obtained in the post-processing of observations at two frequencies

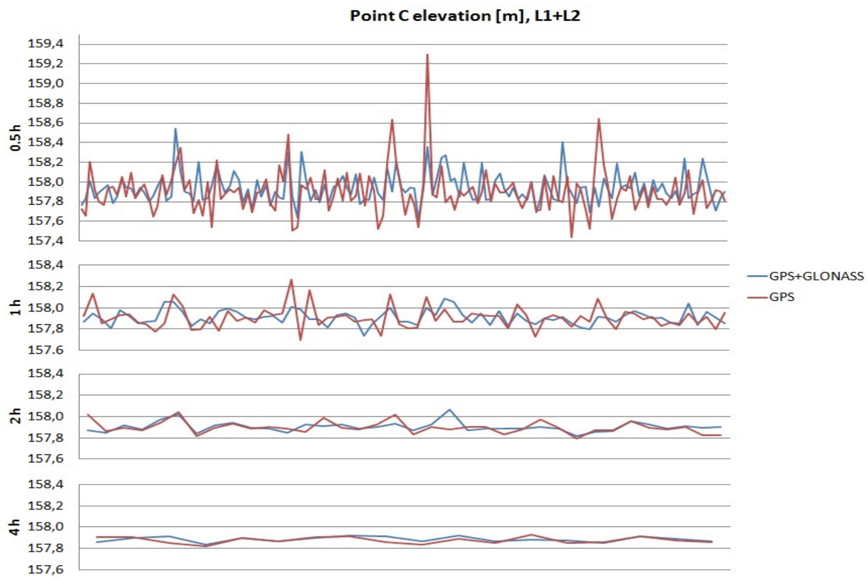

Fig. 8. Elevation of point C obtained in the post-processing of observations at two frequencies

The impact of the length of observation session is clearly visible both on the diagrams of flat coordinates and of elevation (Fig. 3, 4, 5, 6, 7, 8). The determined positions are less-dispersed as the observation sessions become longer. The relationship becomes more apparent in the *GPS+GLONASS* for short sessions. The results presented in Fig. 4, 6, 8 show that adding observations from the *GLONASS* system did not significantly improve the precision of the elevation determination. A comparison of analogous diagrams made for points A, B and C shows the significant effect of terrain obstacles, neighbouring on the measurement site, on the precision of determination of the three-dimensional position of a *GNSS* receiver.

Results of the post-processing of observations made at frequency *L1* are shown in table 4.

Tab. 4. Standard deviations and maximum deviations for the post-processing of *L1*

L1			0.5 h		1 h		2 h		4 h	
			σ	max dev.	σ	max dev.	σ	max dev.	σ	max dev.
Point A	North	*GPS+GLONASS*	0.443	1.486	0.401	1.204	0.362	1.115	0.224	0.476
		GPS	0.427	1.189	0.386	1.095	0.316	0.859	0.207	0.409
	East	*GPS+GLONASS*	0.309	1.088	0.287	0.974	0.267	0.901	0.196	0.525
		GPS	0.234	0.691	0.207	0.590	0.190	0.468	0.155	0.286
	Height	*GPS+GLONASS*	0.942	3.665	0.877	2.940	0.714	2.439	0.613	1.670
		GPS	0.844	2.449	0.789	2.264	0.627	1.677	0.550	1.147
Point B	North	*GPS+GLONASS*	0.539	1.693	0.454	1.154	0.360	1.101	0.207	0.386
		GPS	0.527	1.585	0.439	1.112	0.340	0.745	0.219	0.480
	East	*GPS+GLONASS*	0.334	1.047	0.307	0.981	0.278	0.877	0.200	0.458
		GPS	0.305	0.785	0.277	0.626	0.245	0.501	0.183	0.293
	Height	*GPS+GLONASS*	1.093	4.064	0.973	3.186	0.740	2.328	0.627	1.681
		GPS	0.936	2.802	0.828	2.066	0.606	1.382	0.513	1.023
Point C	North	*GPS+GLONASS*	0.586	1.685	0.493	1.317	0.397	0.951	0.223	0.520
		GPS	0.668	3.169	0.470	1.433	0.399	1.051	0.302	0.860
	East	*GPS+GLONASS*	0.391	1.346	0.356	1.072	0.326	1.049	0.235	0.564
		GPS	0.353	2.044	0.284	0.951	0.258	0.673	0.196	0.322
	Height	*GPS+GLONASS*	1.304	5.093	1.098	4.431	0.874	2.044	0.629	1.482
		GPS	1.066	3.085	0.907	2.279	0.771	1.566	0.584	1.255

Standard deviations in this variant are significantly higher than the deviations obtained in the post-processing of two-frequency measurements and they range from approx. 0.30 m for easting to over 1 m for elevation. Extending the measurement session did not significantly affect either this value or the maximum deviation of the coordinates from the “real” value. Adding the signals from the *GLONASS* system provided results which are in most cases worse than those obtained in post-processing of only *GPS* signals, for both standard and maximum deviation. As mentioned earlier this can be due to a lower accuracy of *GLONASS* corrections that have to be applied in post-processing.

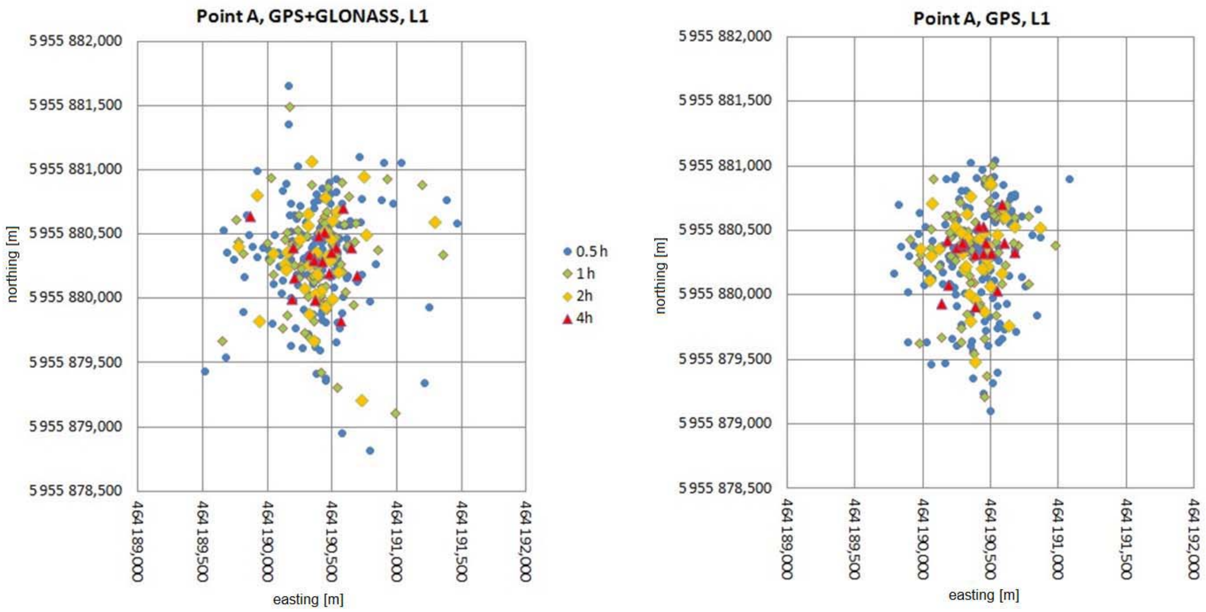

Fig. 9. *UTM* coordinates of point A obtained in the post-processing of observations at one frequency

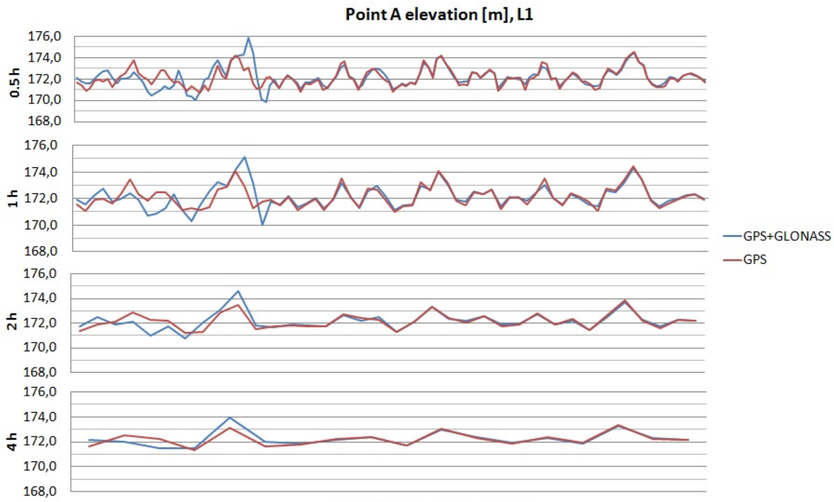

Fig. 10. Elevation of point A obtained in post-processing of observations at one frequency

An analysis of the diagrams 9, 10, 11, 12, 13, 14 showing the results of determinations of coordinates in post-processing at one frequency has confirmed the conclusions based on the results shown in table 4. The diagrams with horizontal coordinates are stretched in the north-south direction. There is no visible improvement of the precision as the duration of sessions extends, and using signals from the *GLONASS* system in the post-processing worsened the results in almost all cases. The diagrams do not show any significant effect of terrain obstacles on the precision, as was the case in measurements performed at two frequencies.

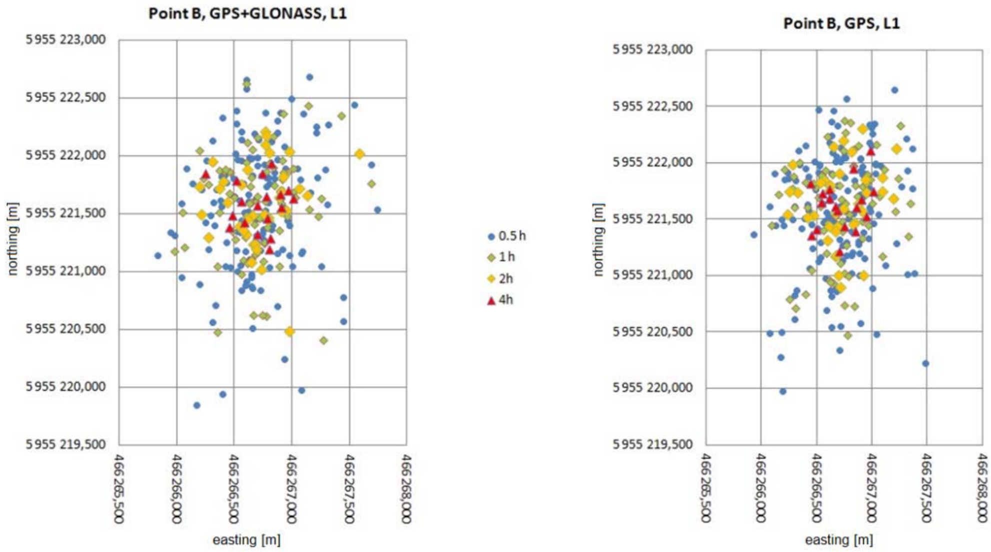

Fig. 11. *UTM* coordinates of point B obtained in the post-processing of observations at one frequency

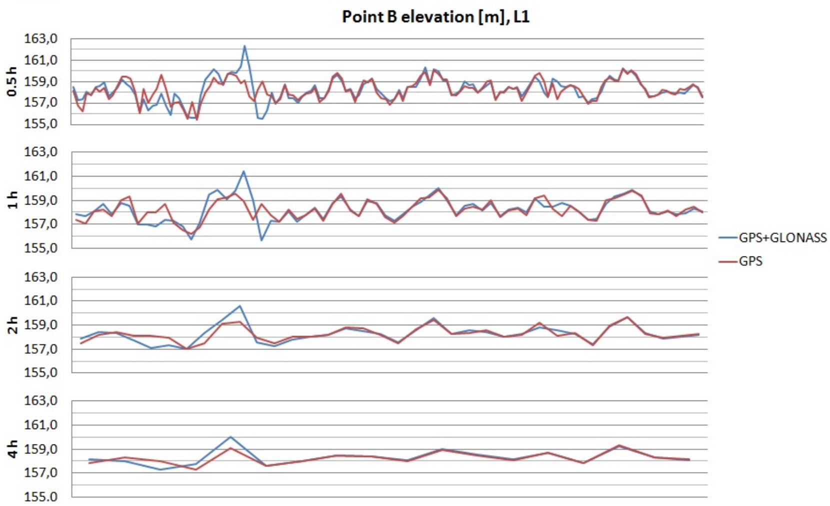

Fig. 12. Elevation of point B obtained in the post-processing of observations at one frequency

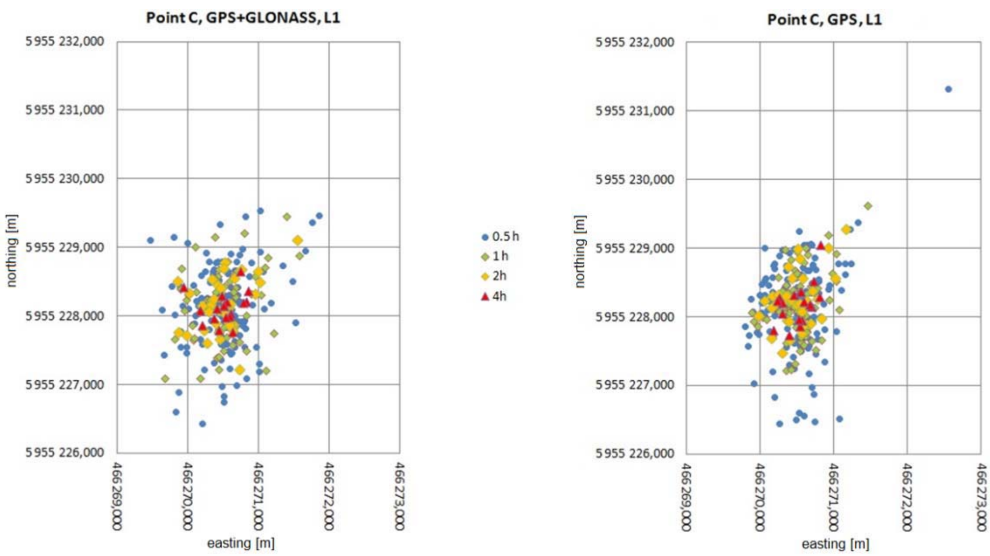

Fig. 13. *UTM* flat coordinates of point C obtained in the post-processing of observation L1

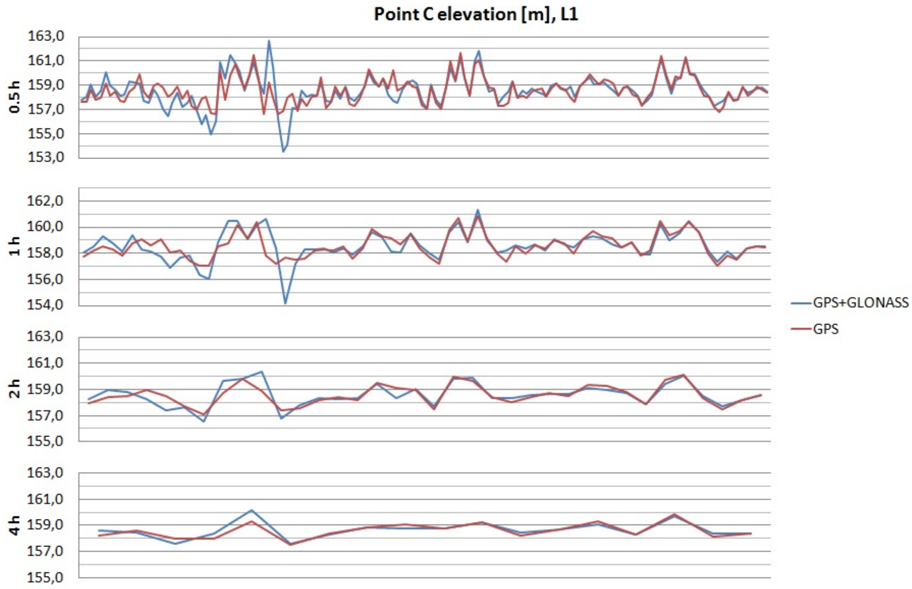

Fig. 14. Elevation of point C obtained in the post-processing of observations at one frequency

5. SUMMARY AND CONCLUSIONS

This paper examined the effect of the duration of a measurement session and of using observations from the *GLONASS* system on the measurement precision in different terrain conditions. An analysis was also performed of the precision of position determination from measurements performed at one or two frequencies and the possibility of automated post-processing of observations with the *CSRS-PPP* service.

The results indicate that under good observation conditions (an unobscured horizon), with two observational frequencies, it is possible to achieve a precision of several centimetres after 2 hours of observation, and the standard and maximum deviations for the northing coordinate obtained in the post-processing of *L1+L2* is approximately twice smaller than the easting and the elevation. This occurs in each time variant and it is manifest mainly at point A with the best measurement conditions. The addition of signals from the *GLONASS* system to the observations performed at two frequencies improved the results for short sessions, especially at points with limited visibility of the horizon (B, C); however the maximum deviations of coordinates from the "real" values increased in many cases (in four-hour sessions in almost all cases). For long sessions (4h) the standard deviations also slightly increased in the *GPS+GLONASS* variant.

When observations were performed at one frequency for 30 minutes, the precision of 0.30 – 0.50 m was achieved for the horizontal coordinates and approx. 1 m for the elevation (standard deviation). The values improved slightly with increased duration of a session, but only four-hour observations reduced the standard deviation by half. The northing in this case had a greater deviation. Adding signals from the *GLONASS* system to the post-processing of observation in general worsened the results obtained in all three points (standard deviation), only slightly reducing the maximum deviation in some cases.

LITERATURE:

Alcay S., Inal C., Yigit C. O. (2012): Contribution of GLONASS Observations on Precise Point Positioning. FIG Working Week 2012 Rome, Italy, 6-10 May 2012.

Bisnath S., Gao Y., (2008): Current State of Precise Point Positioning and Future Prospects and Limitations. International Association of Geodesy Symposia 133.

Bisnath S., Wells D., Dodd D. (2003): Evaluation of commercial carrier phase- based WADGPS services for marine applications. Proceedings of ION GPS/GNSS 9-12 September 2003, Portland, Oregon.

Cai Ch., Gao Y., (2007): Precise point positioning using combined GPS and GLONASS observations. *Journal of Global Positioning Systems*, 6, 1, 13-22.

Hofmann-Wellenhof, B., Lichtenegger, H. and Wasle, E. (2008): GNSS: Global Navigation Satellite Systems – GPS, GLONASS, GALILEO & more, SpringerWienNewYork.

Huber K., Heuberger F., Abart Ch., Karabatic A., Weber R., Berglez P. (2010): PPP: Precise Point Positioning – Constraints and Opportunities. FIG Congress 2010, 11-16 April 2010 Sydney, Australia.

Kouba J., Héroux P., (2001): Precise point positioning using IGS orbit and clock products. *GPS Solutions*, 5, 2, 2001, 12-28.

Mireault Y., Tétreault P., Lahaye F., Héroux P., Kouba J. (2008): Online Precise Point Positioning. *GPS World*, September 2008, 59-64.

Rizos C., (2010): Making sense of the GNSS techniques. *Manual of Geospatial Science and Technology*, 2nd edition, Taylor & Francis, 173-190.

Rizos C., Janssen V., Roberts C., Grinter T., (2012): Precise Point Positioning: Is the Era of Differential GNSS Positioning Drawing to an End? FIG Working Week 2012 Rome, Italy, 6-10 May 2012.

Stępniak K., Wielgosz P., Paziewski J., (2012): Badania dokładności pozycjonowania techniką PPP w zależności od długości sesji obserwacyjnej oraz wykorzystanych systemów pozycjonowania satelitarnego. Biuletyn WAT Vol. LXI, Nr 1, 429-450.

Van Der Marel H., De Bakker P., (2012): Single versus Dual-Frequency Precise Point Positioning. What are the tradeoffs between using L1-only and L1+l2 for PPP? *InsideGNSS*, vol. 7, no. 4, 30-35.

Zumberge, J. F., M. B. Heflin, D. C. Jefferson, M. M. Watkins, and F. H. Webb (1997): Precise Point Processing for the Efficient and Robust Analysis of GPS Data from Large Networks. *Journal of Geophysical Research: Solid Earth*, 102(B3), 5005-5017.

Received: 2013-05-27,

Reviewed: 2013-06-21,

Accepted: 2013-07-04.